



Sulforaphane, a Chemopreventive Compound Induces Necrotic Behavior and Inhibits S-phase of Cell Cycle in Human Kidney Cells *in Vitro*

Guzin Gokay^{1,2*}, Beyza Goncu^{2,3}, Sezen Atasoy⁴, Nur Ozten Kandas⁵, Aydan Dag⁶

1. Bezmialem Vakif University, Health Sciences Institute, Department of Biotechnology, Istanbul, Turkey.

2. Bezmialem Vakif University, Experimental Research Center, Istanbul, Turkey.

3. Bezmialem Vakif University, Vocational School of Health, Department of Medical Laboratory Techniques, Istanbul, Turkey.

4. Bezmialem Vakif University, Faculty of Pharmacy, Biochemistry, Istanbul, Turkey.

5. Bezmialem Vakif University, Faculty of Pharmacy, Pharmaceutical Toxicology, Istanbul, Turkey.

6. Bezmialem Vakif University, Faculty of Pharmacy, Pharmaceutical Chemistry, Istanbul, Turkey.

Article type:**ABSTRACT**

Original Article

Sulforaphane (SFN) is an organosulfur product of found isothiocyanates in vegetables. The chemopreventive effects of SFN have revealed that there is a link between excessive consumption of SFN-rich vegetables and cancer formation without possible toxicological consequences. We aimed to evaluate the cellular outcome of SFN from a toxicological perspective, particularly for renal cells including clear cell adenocarcinoma (769-P) and human embryonic renal epithelial (293T) cells. The viability/cytotoxicity experiments were performed with methyl thiazole diphenyl tetrazolium (MTT) and lactate dehydrogenase (LDH) assays. IC₅₀-dependent, non-cytotoxic concentrations were used for the determination of cell cycle status and apoptosis by using flow cytometry and western blot. A certain concentration of SFN effectively altered apoptotic/necrotic behavior in 769-P compared to the control group 293T. Cell cycle status remained stable while showing a decreased proliferation profile for 769-P cells. The percentage of the S phase from the cell cycle in 293T cells significantly reduced without affecting proliferation status. The use of SFN as an alternative to traditional treatments might be considered for the battle against renal cell carcinoma but the current findings showed that caution should be applied particularly for renal cells. Our study will provide a basis for future *in vivo* studies to support traditional cancer therapies.

Received:

2022.04.07

Revised:

2023.01.01

Accepted:

2023.01.23

Pub Online:

2023.02.01

Keywords: Apoptosis, cell cycle, kidney cancer, sulforaphane, 293T cells, 769-P cells

Cite this article: Gokay. G. Sulforaphane, a Chemopreventive Compound Induces Necrotic Behavior and Inhibits S-phase of Cell Cycle in Human Kidney Cells *in vitro*. *International Journal of Molecular and Cellular Medicine*. 2022; 11(2):104-116. **DOI:** 10.22088/IJMCM.BUMS.11.2.104



© The Author(s).

Publisher: Babol University of Medical Sciences

This work is published as an open access article distributed under the terms of the Creative Commons Attribution 4.0 License (<http://creativecommons.org/licenses/by-nc/4>). Non-commercial uses of the work are permitted, provided the original work is properly cited.

***Corresponding Author:** Guzin Gokay

Address: Adnan Menderes Bulvari, Vatan Caddesi, 34093, Fatih, Istanbul, Turkey.

E-mail: gokayguzin@gmail.com

Introduction

Phytochemicals are herbal chemicals that are spontaneously produced in fruits, vegetables, or cereals. They have been widely studied for their chemopreventive characteristics and many of them are beneficial for healthy living (1). Their comprehensive effects and therapeutic value have driven phytochemicals as interesting tools for cancer treatment. Despite their potential and easy accessibility, they suffer from major drawbacks such as instability, inadequate bioavailability, and limited absorption by the cell membrane (2). Thus, the formation of appropriate strategies to promote the use of phytochemicals is crucial.

Sulforaphane [1-Isothiocyanato-4-(methylsulfonyl) butane] (SFN) is a naturally-occurring isothiocyanate that is derived from broccoli and other crucifers. SFN results from the hydrolysis of glucosinolate-type glucoraphanin with endogenous myrosinase enzyme (3). The highest levels of glucosinolate are mostly found in broccoli sprouts. Several studies investigating SFN revealed that chemoprevention mechanisms of SFN affected various molecular interactions, and played a role in carcinogenesis (4). Anti-inflammatory (5), anti-oxidant (6), anti-apoptotic (7), protection against tumor development and suppression effects(8), and anticancer effects (9) were shown for SFN. SFN is not a direct anti-oxidant or pro-oxidant agent itself, but rather indirectly affects the anti-oxidant capacity and ability to cope with oxidative stress (10). Although a considerable amount of literature has been carried out on SFN, the full understanding of its potential in a medicinal application for the treatment and prevention of cancer is still restricted. To date, there has been little agreement on what is the suitable intake for providing effective doses of herbal products or dietary supplements (11). Preliminary experimental evidence on SFN for the treatment of cancer suggested that SFN repressed angiogenesis, the transformation of benign to malignant tumors and metastases. However, along with these toxicity studies, no previous study has investigated the effects of SFN on renal cells.

Renal cell carcinoma (RCC) is the most common solid lesion that occurs in the kidney, accounting for 90% of all renal malignancies (12). There are many factors contributing to the etiology of RCC, nevertheless, the cause remains unknown (13). Around 2-3% of all cancers in adults are associated with RCC. Among all of the RCC cases, clear cell RCC (ccRCC) is the most common histological type (14). It is considered slowly progressive, but still, some of the cases have shown to be aggressive and even metastasized (15). The absence of early markers, nonspecific symptoms, and poor diagnosis may require aggressive treatment options, as well as distant metastases (16). Management of the disease focuses on surgery and ablation as chemotherapy is not completely effective, especially for ccRCC (12). Surprisingly, a particular study showed that resistance development was delayed against RCC via SFN-mTOR inhibitor (everolimus) combined treatment *in vitro* (17).

There is a general lack of scientific data about how SFN may affect cancerous and non-cancerous renal cells. This study aimed to obtain a preliminary analysis of SFN on renal cell toxicity. The cytotoxic effects of possible SFN-mediated cell damage between clear cell adenocarcinoma (769-P) and renal epithelial embryo (293T) cell lines were determined using methyl thiazole diphenyl tetrazolium (MTT) and lactate dehydrogenase (LDH) assays. Cell cycle and cell death progression were analyzed and apoptotic-necrotic behavior was confirmed with western blot.

Materials and Methods

Cell Culture

Human renal cell adenocarcinoma cell line 769-P and human embryonic kidney epithelial cell line 293T were obtained from American Tissue Culture Collection (ATCC, VA, USA). Cells were grown in RPMI 1640 (Gibco, Thermo Fisher Scientific, MA, USA) for 769-P, DMEM (Gibco, Thermo Fisher Scientific, MA, USA) for 293T supplemented with 10% fetal bovine serum (FBS) (Gibco, Thermo Fisher Scientific, MA, USA) and 1% penicillin/streptomycin (Gibco, Thermo Fisher Scientific, MA, USA) at 37°C with 5% CO₂. Cells were cultured in 25 cm² flasks (Isolab GmbH, Germany) and harvested with 0.05% trypsin-EDTA (Gibco, Thermo Fisher Scientific, MA, USA) when they reached 80% confluence.

Preparation of SFN Dilutions

Dilutions of the commercially purchased SFN (CAS 4478-93-7, Cayman, Michigan, USA) were prepared using DMEM and RPMI 1640 complete medium for each cell type. 141.0039 mM stock SFN was dissolved in 2 mL ethanol. Serial dilutions using growth medium were prepared from the stock SFN solution at 200 µM, 100 µM, 50 µM, 25 µM, 12.5 µM, 6.25 µM, 3.125 µM, 1.56 µM, 0.78 µM, 0.39 µM, 0.19 µM, and 0.095 µM final concentrations.

Analysis of the Cytotoxicity

Determination of the cell viability and toxicity were performed by MTT and LDH assays, respectively. Cultured cells were seeded into flat bottomed 96 well plates with a density of 5x10³ cells/well and allowed to attach for 24h. Then, the concentration series of SFN was added to cells in triplicates and incubated for 24h, 48h, and, 72h for MTT assay. 10 µL of MTT (Invitrogen, Thermo Fisher Scientific, MA, USA) (5 mg/mL in PBS) was added to each well and the plates were incubated for 4 h at 37°C in the dark. Finally, for dissolving formazan crystals, 100 µL of DMSO was added to each well and the absorbance at 540 nm was measured. The relative viability percentage was calculated from the following equation: Relative percent cell viability = (A_{test}/A_{control}) x 100%. (A_{test} is the absorbance of the sample treated cells and A_{control} is the absorbance of the untreated cells). Quantification of the cellular cytotoxicity was performed as explained above to establish an LDH assay (Pierce LDH Cytotoxicity Assay Kit, Thermo Fisher Scientific, MA, USA) according to the manufacturer's protocol. Briefly, after the treatment with SFN, a 50 µL medium was collected for the released LDH, transferred to a new 96 well plate, mixed with a 50 µL reaction mixture, and incubated for 30 min at room temperature in the dark. Reactions were stopped by adding a 50 µL stop solution and absorbance at 490 nm and 680 nm was measured using a multiplate reader (Biotek Synergy H1 Hybrid Multi-Mode). For calculating the percentage of the cytotoxicity, LDH activity of the spontaneous LDH release control (water-treated) was subtracted from the treated LDH sample activity, divided by the total LDH activity [(Maximum LDH Release Control activity) – (Spontaneous LDH Release Control activity)], and multiplied by 100.

Analysis of Cell Death and Cell Cycle

Apoptosis and cell cycle profiles of the cells were determined using Muse Cell Analyzer (Millipore, MA, USA) according to Annexin V/7'AAD & Dead Cell Kit (#MCH100105) and Cell Cycle Kit (#MCH100106) assay protocols. Briefly, 769-P and 293T cells were cultured in a 24-well plate with a density of 50 x 10³ cells/well and allowed to attach for 24h in a 2 mL medium. To further evaluate SFN

treatments, flow cytometric analysis was carried out using only 25 μ M, 12.5 μ M, 6.25 μ M, 3.125 μ M, 1.56 μ M, and, 0.78 μ M concentrations, based on dose and time response results of the cytotoxicity analysis. As a result of higher concentrations causing a dramatic decline in the viability, to achieve SFN activities, cells were treated for 48h with 25 μ M, 12.5 μ M, 6.25 μ M, 3.125 μ M, 1.56 μ M, and, 0.78 μ M SFN dilutions. After the incubation, cells were collected for apoptosis assay. 100 μ L of Annexin V/7'AAD & Dead Cell Reagent and 100 μ L of cell suspension were added to a tube and incubated in dark for 20 min at room temperature. Also for cell cycle analysis, cells were collected after the incubation and washed with 1X phosphate-buffered saline (PBS). After centrifuging at 300 x g for 5 min, cells were fixed in 1 mL 70% cold ethanol at -20 °C for 3 h and washed with 1X PBS. 200 μ L of cell suspension and 200 μ L of Muse cell cycle reagent were added to the tube and incubated in dark for 20 min at room temperature. Quantification of both assays was performed using the analyzer.

Western Blotting

Both cell lines were incubated with 12.5 μ M, 6.25 μ M, and 3.125 μ M SFN for 48 h upon considering their half-maximal inhibitory concentration values and cell death and cell cycle analysis results. After the incubation, the cells were washed with 1X PBS and for obtaining total protein extracts, 1 x 10⁶ cells were lysed in 100 μ L complete RIPA lysis buffer (containing 5 μ L phenylmethylsulfonyl fluoride, 5 μ L sodium orthovanadate solution, and 5 μ L protease inhibitor cocktail) (Santa Cruz, TX, USA). The cell suspension was frozen at -80°C and the supernatant was collected after centrifuging for 15 minutes at 13000 x g. Total protein concentrations were measured using Qubit™ Protein Assay Kit (Invitrogen, Thermo Fisher Scientific, MA, USA). 30 μ g sample of total protein was prepared using 2X Laemmli sample buffer (Bio-Rad, CA, USA) and separated on 4–12% polyacrylamide gel. Separated proteins were transferred to 0.2 μ m PVDF membranes (Bio-Rad, CA, USA) using a semi-dry system in a 1X transfer buffer at 1 ampere, 25 voltage for 10 minutes with the Trans-Blot Turbo Transfer System (Bio-Rad, CA, USA). After blocking PVDF membranes at room temperature with TBST (Tris Buffered Saline with 0.02% Tween-20) containing 5% nonfat milk, the membranes were probed with primary antibodies against β -actin (1:1000 dilution, #4967, Cell Signaling, MA, USA), poly ADP-ribose polymerase (PARP) (1:1000 dilution, #9542, Cell Signaling, MA, USA) and proliferating cell nuclear antigen (PCNA) (1:2000 dilution, #2586, Cell Signaling, MA, USA). For secondary antibodies, anti-rabbit IgG and anti-mouse IgG HRP-linked antibodies (1:3000 dilution, Cell Signaling, MA, USA) were used. Detection of the signal from the blots was developed using the Enhanced Chemiluminescence (ECL) detection kit (Advansta, CA, USA). Densitometric analysis of band densities was measured using Image-J and normalized against that of β -actin in each sample.

Statistical Analysis

The statistical analysis was conducted using a one or two-way analysis of variance (ANOVA) followed by Dunnett's test for multiple comparisons and Student's t-test for comparisons between groups when necessary. Furthermore, *post-hoc* pairwise comparisons included a two-by-two basis, and all the outcomes from all assays were involved and additionally the concentrations versus untreated groups and/or time intervals versus concentrations and/or between cell types versus all were analyzed. All data are presented as the mean \pm SD, with a significance level of $p \leq 0.05$. Western blot images were quantified

densitometrically and normalized using an internal control (β -actin) by ImageJ. All results were evaluated using GraphPad Prism v8.3 (GraphPad Software, CA, USA).

Results

Cytotoxic Effects of SFN

The half-maximal inhibitory concentration values (IC_{50}) of SFN in the treated cell lines were calculated by AAT Bioquest using MTT assay data (18).

The IC_{50} of SFN for 293T cells was 19.3 μ M, 13.5 μ M, and 6.2 μ M, and for 769-P cells, the IC_{50} was found at 19 μ M, 11.2 μ M, and 15.1 μ M for each time interval, respectively. The survival rates including viability changes and the cytotoxicity of 293T and 769-P cells after 24, 48, and 72 h treatments with SFN are presented in Figure 1. The cell viability for both cell lines decreased with increasing concentrations of SFN when compared to the untreated group. On the one hand, despite the IC_{50} , approximately 50% viability was predicted at a concentration between 25 to 50 μ M (69% and 32% respectively) for 24 h of treatment with SFN (Figure 1A). Besides, after 48 h treatment, the viability showed significant changes at 12.5 μ M (46.2%) concentration ($p=0.0109$). Viability continued to decrease as the duration of treatment was prolonged, and similar results with the IC_{50} value were valid only for 24 and 48 hours. Cellular cytotoxicity levels did not show significant differences between 0.095 μ M and 50 μ M concentration rates when compared with untreated groups (Figure 1B) and this indicated that cytotoxicity was dose and time-dependent.

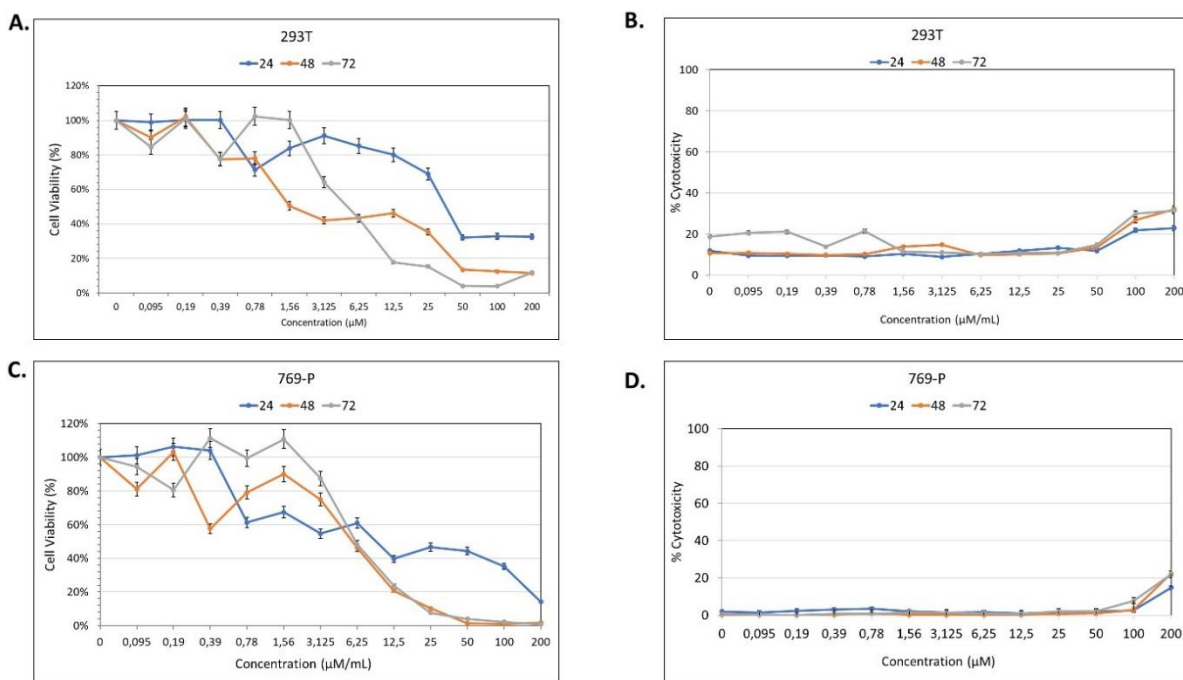


Fig.1. Cell viability from MTT assay and cytotoxicity results from LDH assay Results of SFN treated 293T cells (A.) and SFN treated 769-P cells (C.) by MTT assay following 24, 48, and 72 hours. **B.** Results of SFN treated 293T cells and **D.** Results of SFN treated 769-P cells by LDH assay following 24, 48, and 72 hours. All experiments were performed in triplicate and the results were analyzed and presented as mean \pm standard deviation. MTT: 3-(4,5-dimethylthiazol-2-yl)-2,5-diphenyltetrazolium bromide, LDH: lactate dehydrogenase, SFN: sulforaphane [1-Isothiocyanato-4-(methylsulfonyl)butane].

On the other hand, the 769-P cells showed a decreasing viability pattern for all incubation times when incubated with 6.25 μ M or higher concentrations (Figure 1C) over time. Considering the IC_{50} value approximately 50% viability was found at 6.25 μ M and that provided a viability value of 60.9% for 769-P cells after 24 h. Besides, at 48 h of treatment showed 46.2% viability for the same concentration (6.25 μ M). The higher concentrations of SFN also include 50, 100, and 200 μ M, and these concentrations underwent almost complete cell killing after 48 h incubation for 769-P cells (Figure 1C). The LDH activity measurements provided that 769-P cells incubated with 25, 50, 100, and 200 μ M SFN affected cell toxicity, yielding nearly similar trends to the MTT assay (Figure 1D).

To further evaluate whether the treatment of SFN affected cells, the following experiments were carried out using 12.5 μ M, 6.25 μ M, and 3.125 μ M SFN concentrations at 48 h. After IC_{50} determination and comparison of MTT and LDH assays, a 48-hour treatment was preferred and decreased dose titration starting from the IC_{50} values (closest working concentration was found at 12.5 μ M) as a high concentration limit for both cell lines. Further experiments were performed with 12.5 μ M, 6.25 μ M, and 3.12 μ M respectively.

Effect of SFN on the Induction of Apoptosis

To identify the effects of SFN on cellular damage and death in 293T and 769-P cells, the Annexin V/7'AAD method was performed using 12.5 μ M, 6.25 μ M, and 3.125 μ M SFN after 48 h of treatment. The cell profile was determined as live, early apoptotic, late apoptotic/dead, and total apoptotic profiles after treatment with SFN. Raw profiles were complied in Supplementary Figure 1. The changes in early and total apoptotic cell percentages demonstrated that non-cancerous cells showed altered dead cell profile after incubation with the same concentration (Figure 2A), also 769-P cells after 48h incubation with 12.5 μ M SFN led cancer cells to death (Figure 2D). A significant increase in the early apoptosis cell profile was observed in 293T cells at a concentration of 6.25 and 12.5 μ M SFN ($p= 0.024$ and $p<0.001$, respectively) when compared to the untreated group. In 769-P cells, a significant increase only occurred for 12.5 μ M SFN ($p= 0.005$), when compared with the untreated group. This observation suggested that a higher concentration of SFN such as 12.5 μ M could induce cell death by increasing the total apoptotic cell profile for cancer cells, and also for non-cancerous cells.

To distinguish the mechanism of cell death, apoptosis and necrosis-related poly ADP-ribose polymerase (PARP) protein expression levels by western blot analysis were used. Untreated 293T cells expressed hardly noticeable cleaved PARP. On the other hand, SFN treatments led 293T cells to undergo cell damage, especially for 12.5 μ M SFN (Figure 2B). As shown in Figure S2D, all SFN treatments induced elevated necrotic PARP protein levels than the untreated group. These results also matched those observed in flow cytometric studies. Protein expression levels presented in both blot images showed that total PARP was cleaved in fragments of 89 and 50 kDa (apoptosis and necrosis indicator, respectively) during SFN treatments (Figures 2B and 2E). Changes in total and cleaved PARP protein levels were also analyzed in 769-P cells. As described above, untreated 769-P cells also showed no PARP cleavage. Contrarily, 48h treatment of cells to SFN resulted in increments of necrotic cleavage products (Figure 2E). SFN treatments provoked a major loss of total PARP and protein expression levels were found significantly decreased, where necrotic cleavage products were raised at all concentrations of SFN (Figure S2A) ($p <0.001$).

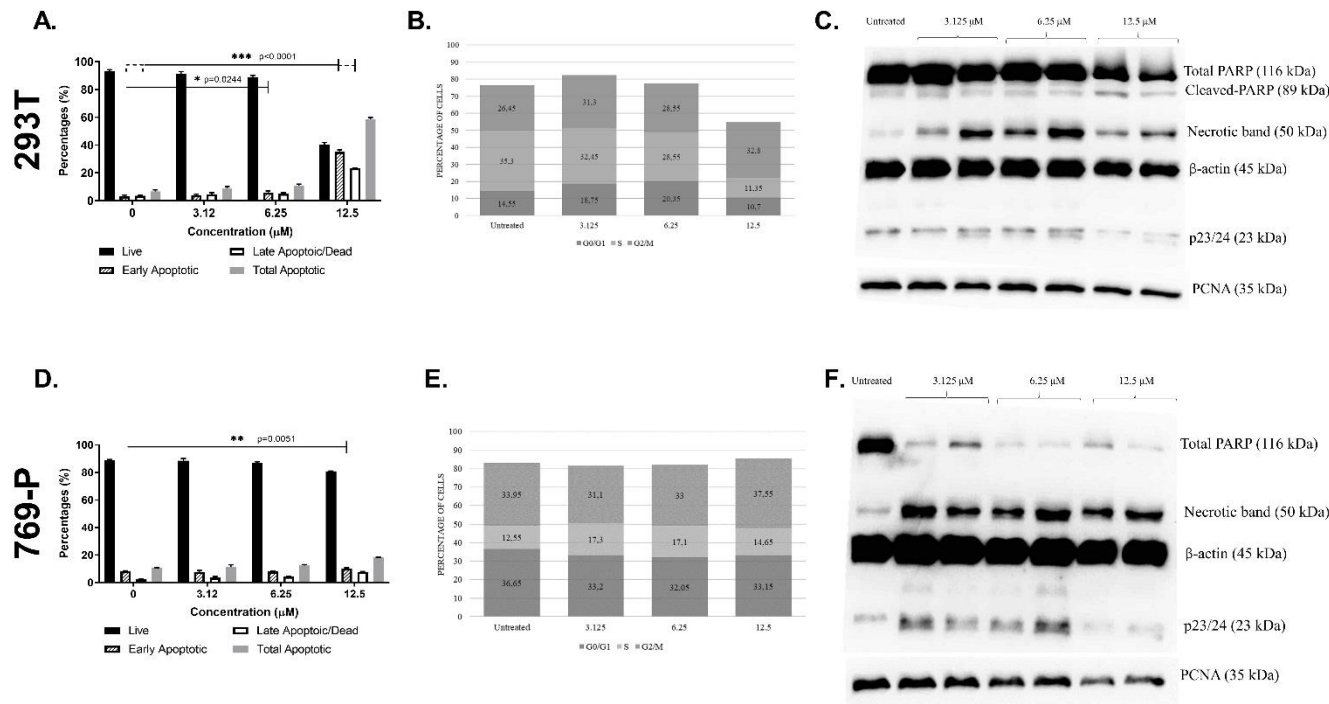
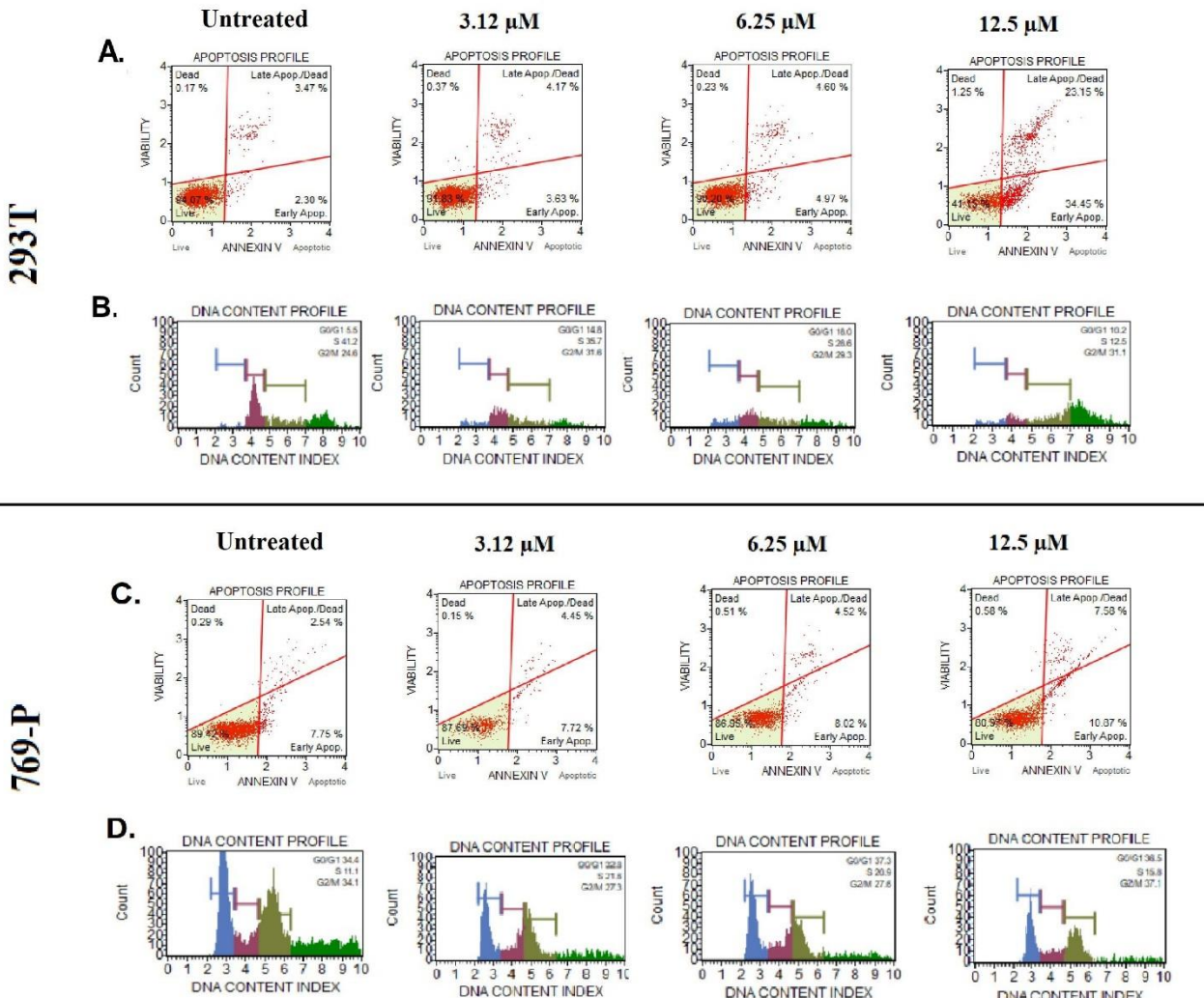


Fig.2. For apoptosis analysis, 293T (A) and 769-P (D) cells were treated with 3.125 μ M, 6.25 μ M, and 12.5 μ M SFN. Flow cytometry analysis for 293T cells showed to induce early apoptosis at 6.25 and 12.5 μ M of SFN ($p= 0.024$ and $p<0.001$, respectively). Flow cytometry analysis for 769-P cells showed to induce early apoptosis at 12.5 μ M of SFN ($p=0.005$). Results of cell cycle analysis of 293T (B) and 769-P (E) cells treated with 12.5 μ M, 6.25 μ M, and 3.125 μ M SFN. The percentage of cells in the G0/G1, S, and G2/M phases was obtained by flow cytometer. 293T cells treated with indicated concentrations (μ M) of SFN for 48 h showed 12.5 μ M SFN significantly decreased the percentage of the cells in the S phase ($p=0.001$). 769-P cells treated with indicated concentrations (μ M) of SFN for 48 h showed no significant changes in the cell cycle profile ($p>0.05$). Western blot images of PARP, its cleavage products, and, PCNA protein expressions in 293T cells (C) and 769-P cells (F) were determined using chemiluminescent methods and relative protein quantification was made by densitometric analysis. Apoptosis and cell cycle experiments were performed in triplicate, the western blot method was performed in duplicate and the results were analyzed with one-way or two-way ANOVA when necessary and presented as mean \pm standard deviation. μ M: micromolar, SFN: sulforaphane [1-Isothiocyanato-4-(methylsulfonyl)butane], PARP: poly ADP ribose polymerase, PCNA: Proliferating cell nuclear antigen.

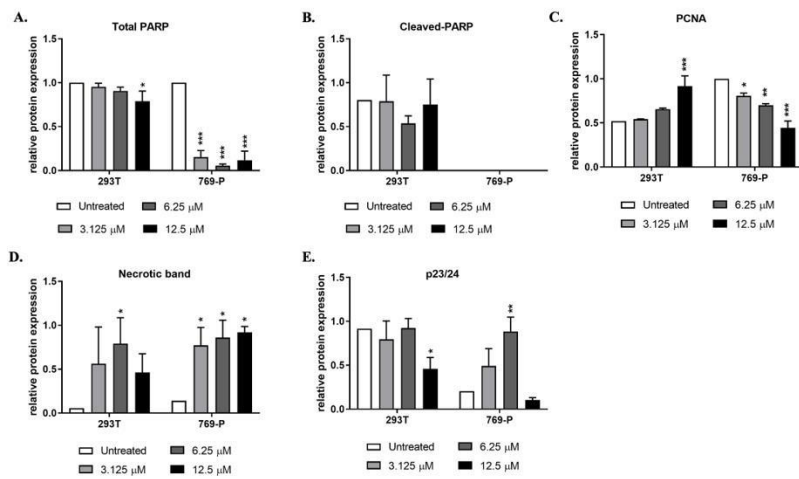
Effect of SFN on Cell Cycle

To assess whether SFN promotes cellular growth inhibition via alterations in the cell cycle, the effects on cell cycle distribution were examined using a flow cytometer. Population stages for 293T and 769-P cells were determined after 48 h treatment with 12.5 μ M, 6.25 μ M, and 3.125 μ M SFN (Supplementary Figure 1B and 1D, respectively). The results from the four checkpoints that exist in the cell cycle (G0 / G1, S, and G2 / M) of 769-P and 293T cells were shown in Figures 2C and 2F, respectively. Treatments with SFN did not affect the percentage of cell numbers in the G0/G1, S, and G2/M phases in 769-P cells. No significant differences were found in these measurements (Figure 2E). Interestingly, there were significant differences in the ratios of the cell cycle in 293T cells, SFN significantly caused a decline in the 293T cells at the S phase ($p=0.0014$) (Figure S2B). The percentage of cells in the S phase with no treatment (untreated)

exhibited 35.3% and decreased to 11.35% when treated with 12.5 μ M SFN. These results suggested that 12.5 μ M SFN is associated with S-phase in 293T cells compared to the untreated cells. In addition, PCNA protein expression analysis was carried out to confirm the changes in the S phase. Further analysis showed that, as expected, PCNA protein levels were elevated at 12.5 μ M SFN for 293T cells, and declined for 769-P cells (Figure 2B, and Figure 2E,Supplementary and Figure 2C, respectively).



Supplementary Fig.1. For analysis of cell death, 293T (A) and 769-P (C) cells were treated with 3.125 μ M, 6.25 μ M, and 12.5 μ M SFN. Flow cytometry results were presented as the apoptosis profiles of three independent experiments of living, early apoptotic, and total apoptotic after 48 h treatment. The gating was adjusted according to the untreated sample and the representative scatterplots were presented as the percentage of cells that were viable (Ann-V $^-$ 7-AAD $^-$), early apoptotic (Ann-V $^+$ 7-AAD $^-$), late apoptotic (Ann-V $^+$ 7-AAD $^-$), and dead (Ann-V $^-$ 7-AAD $^+$). For cell cycle analysis, 293T (B) and 769-P (D) cells were treated with 3.125 μ M, 6.25 μ M, and 12.5 μ M SFN. Flow cytometry results were presented as DNA histograms of cell cycle distributions of three independent experiments after 48 h treatment. Analyzed cells were gated on DNA content and cell size index parameters to determine the G0/G1, S, and G2/M phase (μ M: micromolar, SFN: sulforaphane [1-Isothiocyanato-4-(methylsulfonyl) butane], Ann-V: Annexin V, 7-AAD: 7-aminoactinomycin D).



Supplementary Fig.2. Relative protein expression levels of total PARP (A), cleaved-PARP (B), PCNA (C), necrotic (PARP) band (D), and p23/24 (E) obtained from western blot analysis were presented. Protein expression changes of mentioned proteins in 293T and 769-P cell lines using 3.125 μ M, 6.25 μ M, and 12.5 μ M SFN were calculated as relative values to the reference protein (β -actin). p values were indicated as **p < 0.001, ***p < 0.0001. All experiments were performed in duplicate, and the results were analyzed and presented as mean \pm standard deviation. All p-values were obtained by two-way ANOVA following Dunnet's multiple comparison test. μ M: micromolar, PARP: poly ADP ribose polymerase, PCNA: Proliferating cell nuclear antigen, SFN: sulforaphane [1-Isothiocyanato-4-(methylsulfonyl)butane].

Discussion

Phytochemicals play an important role in preventing and curing cancer through various biological activities. The role of phytochemicals in cancer prevention and treatment via antioxidant & pro-oxidant activity, apoptosis, necrosis, autophagy induction, along regulation of miRNA expression were demonstrated (19).

SFN has been reported to inhibit the cell growth of several cancer types and has been shown to induce apoptosis. Specifically, it is presented as an effective chemopreventive molecule in all *in-vitro*, *in-vivo*, and xenograft models, holding potential for cancer prevention (20). One of the major drawbacks over the years of traditional cancer treatments such as chemotherapy and radiotherapy have systemic toxicity and ineffective regimens. Previous studies have reported that combining SFN with chemotherapy and radiotherapy showing increased sensitivity and therapeutic efficacy for resistant cancer cells. Continuous use of chemotherapeutic agents such as gemcitabine and cisplatin, with SFN, had increased anti-tumor effect and reduced cytotoxicity, even at low doses (21). It was also found that SFN causes cell cycle arrest together with anti-proliferative and apoptotic effects (22). The study of the link between SFN and apoptosis was first determined in HT29 and Caco-2 colon cancer cells, following the definition of caspase activation in LNCaP prostate cancer cells (23, 24). Contrary to the previous reports, SFN had also been shown to inhibit apoptosis, and two published studies described the mechanism of apoptosis for different cell lines except for renal carcinoma cells (4, 25, 26). In 2017, Lan et al. found decreased viability in a dose-dependent manner (at 0-20 μ M concentrations) when treated with SFN for human colon cancer cells (SW480 and

HCT-116) (27). In 2018, Rutz et al. observed that SFN treatment on the A498 renal carcinoma cell line reduced cell proliferation (28). Observed studies demonstrated that the progressive behavior of SFN on cancer cells varies depending on the type (bladder, bone, brain, breast, colon, etc.) of cancer cells (29). Recently, in a study with gastric cancer cell lines (BGC-823 and MGC-803), SFN has been found to significantly suppress cell proliferation by arresting the cell cycle in the S phase and increasing cell apoptosis in a dose-dependent manner. Protein expression results showed that SFN treatment significantly increased the expression levels of p53 (tumor protein, TP53) and p21 (cyclin-dependent kinase inhibitor 1) which directly regulates the S phase transition (30).

There is numerous published study that describes the role of SFN treatment in cancer cell lines except for kidney cells. Therefore we aimed to evaluate the changes in the cell status by apoptosis/ cell cycle, and protein expression changes after treatment with SFN on kidney cancer cells. Current findings in this study, SFN treatment on RCC showed a necrotic behavior which is confirmed by protein expression. Additionally, inhibiting the S phase during the cell cycle when compared to healthy kidney cells. LDH assay demonstrated that 293T cells had low cytotoxic activity, even with higher doses (up to 25 μ M) and for 769-P cells, cytotoxicity had increased over time depending on the increased concentration. Furthermore, the suitable working concentration was approved by IC₅₀ determination. The results of the 48 h SFN treatment showed a more proportional effect during decreased dose titration for viability and cytotoxicity results from both cell lines. Continued experiments were carried out within 48 h of treatment and included concentrations were 12.5 μ M, 6.25 μ M, and 3.12 μ M, respectively. As of note, we were aware that the 6.25 μ M and 12.5 μ M have 30% viability however, the IC₅₀ levels were more reliable and taken into consideration more primarily than MTT and LDH assay results.

In 293T cells, the population profile of early apoptosis showed significant alterations with increased concentration of SFN, however, that increment did not correlate with the total PARP and cleaved-PARP protein expressions. A considerable amount of literature has been published about the activation of proteases that may result in the production of PARP fragments (31). A specific signature of the fragments was detected that involved the type of cell death (31). The molecular weights of cleaved PARP fragments are 89 kDa, 64 kDa, 50 kDa, and 21 kDa or p23/24 kDa (this protein has two overlapping terms) (31). The presence of 89 kDa and 21 kDa fragments correlated with the activation of Caspase-3 and the presence of apoptotic cell deaths. In another study, about 50 kDa and 64 kDa cleaved PARP fragments were related to cathepsin-b and elevated levels of granzyme-b respectively and as a result, the presence of necrotic cell death (31). In this study, the relative PARP and PARP fragment protein expression showed a dose-dependent necrotic response and p23/24 expression had significantly changed when compared with the untreated group. The necrotic band of PARP protein (50 kDa fragment) was found significant at 6.25 μ M concentration in 293T cells, however, the p23/24 protein levels for the same concentration showed no significant differences. Besides, there was a decrease in protein expression for 12.5 μ M concentration. Furthermore, proliferative cell marker PCNA relative protein expression analysis had not found significant changes below 12.5 μ M concentration for 293T cells, while 769-P cells showed a significant decrease in a dose-dependent manner. Although, the cell cycle S-phase population profile was detected to significantly decreased in the 293T cells after treatment with SFN.

In 769-P cells, the early apoptotic cell population was found to significantly increase for the higher SFN concentrations. The dose-dependent changes were also determined for total-PARP and its cleaved products. The outcome of the apoptosis was found to correlate with the relative total PARP protein expression. The necrotic band showed a significantly higher protein expression level for all concentrations. No band seemed for cleaved PARP, however, the p23/24 protein expression was observed in all concentrations, even with the necrotic response. In addition, the PCNA relative protein expression levels significantly decreased by the treatment in a dose-dependent manner. Hence, SFN treatment in 769-P altered effectively apoptotic/necrotic behavior more than in healthy renal cells (293T). Additionally, the cell cycle population profile was found to be affected by SFN treatment but statistical analysis of these changes was not significant. Yet, the population of S-phase increased treatment with higher concentrations without affecting proliferation (according to the relative PCNA protein expression level).

There is a degree of uncertainty about the phytochemicals and their target mechanisms. Most of the phytochemicals reported have an apoptotic effect by caspase induction. Some reports indicated that necrosis may have a role in controlling neoplastic cells by destroying tumor cells. Using phytochemicals while causing necrosis may propose a different strategy, which could enable the development of new drug research against cancer. Most phytochemicals can also affect the mediators that have a role in cell death. Therefore, inducing necrosis and apoptosis synergistically may provide a promising approach (19).

In conclusion, the presented studies so far outlined that SFN could provide an effective and safe chemopreventive phytochemical. The use of SFN as an alternative to traditional regimens might be considered a suitable candidate against kidney cancer. However, the current findings showed that caution should be applied during the use of SFN. As of note, this study has a limitation regarding the lack of healthy adult kidney cells. A comparison between clear cell adenocarcinoma (769-P) and embryonic renal epithelial (293T) cell lines may not adequately suggest comparable outcomes. However, the results of this study provide a basis for future *in vivo* and clinical studies of SFN on renal cells. The susceptibility to kidney cell profile during apoptosis via SFN treatment is dose-dependent, and induced necrotic cell death might play a role. Cell cycle profile and a true reflection of proliferation status are possibly related to the time-dependent manner. Further research should be performed for clarification of the outcome and precise mechanisms.

Acknowledgments

The authors acknowledge Belma Zengin Kurt, Ph.D., and Dilek Ozturk, Ph.D. for providing cell lines used in this study. This work was supported by Bezmialem Vakif University Scientific Research Projects (BAP) Coordination Unit (62017/47).

References

1. Herr I, Buchler MW. Dietary constituents of broccoli and other cruciferous vegetables: implications for prevention and therapy of cancer. *Cancer Treat Rev* 2010;36:377-83.
2. Salama L, Pastor ER, Stone T, et al. Emerging Nanopharmaceuticals and Nanonutraceuticals in Cancer Management. *Biomedicines* 2020;8.

3. Cheung KL, Kong AN. Molecular targets of dietary phenethyl isothiocyanate and sulforaphane for cancer chemoprevention. *AAPS J* 2010;12:87-97.
4. Juge N, Mithen RF, Traka M. Molecular basis for chemoprevention by sulforaphane: a comprehensive review. *Cell Mol Life Sci* 2007;64:1105-27.
5. Lin W, Wu RT, Wu T, et al. Sulforaphane suppressed LPS-induced inflammation in mouse peritoneal macrophages through Nrf2 dependent pathway. *Biochem Pharmacol* 2008;76:967-73.
6. Danilov CA, Chandrasekaran K, Racz J, et al. Sulforaphane protects astrocytes against oxidative stress and delayed death caused by oxygen and glucose deprivation. *Glia* 2009;57:645-56.
7. Yang LP, Zhu XA, Tso MO. Role of NF- κ B and MAPKs in light-induced photoreceptor apoptosis. *Invest Ophthalmol Vis Sci* 2007;48:4766-76.
8. Clarke JD, Dashwood RH, Ho E. Multi-targeted prevention of cancer by sulforaphane. *Cancer Lett* 2008;269:291-304.
9. Gamet-Payrastre L. Signaling pathways and intracellular targets of sulforaphane mediating cell cycle arrest and apoptosis. *Curr Cancer Drug Targets* 2006;6:135-45.
10. Fahey JW, Talalay P. Antioxidant functions of sulforaphane: a potent inducer of Phase II detoxication enzymes. *Food Chem Toxicol* 1999;37:973-9.
11. Socala K, Nieoczym D, Kowalcuk-Vasilev E, et al. Increased seizure susceptibility and other toxicity symptoms following acute sulforaphane treatment in mice. *Toxicol Appl Pharmacol* 2017;326:43-53.
12. Ljungberg B, Bensalah K, Canfield S, et al. EAU guidelines on renal cell carcinoma: 2014 update. *Eur Urol* 2015;67:913-24.
13. Cairns P. Renal cell carcinoma. *Cancer Biomark* 2010;9:461-73.
14. Sanchez-Gastaldo A, Kempf E, Gonzalez Del Alba A, et al. Systemic treatment of renal cell cancer: A comprehensive review. *Cancer Treat Rev* 2017;60:77-89.
15. Brufau BP, Cerqueda CS, Villalba LB, et al. Metastatic renal cell carcinoma: radiologic findings and assessment of response to targeted antiangiogenic therapy by using multidetector CT. *Radiographics* 2013;33:1691-716.
16. Cohen HT, McGovern FJ. Renal-cell carcinoma. *N Engl J Med* 2005;353:2477-90.
17. Juengel E, Euler S, Maxeiner S, et al. Sulforaphane as an adjunctive to everolimus counteracts everolimus resistance in renal cancer cell lines. *Phytomedicine* 2017;27:1-7.
18. Barakat-Walter I, Kraftsik R. Stimulating effect of thyroid hormones in peripheral nerve regeneration: research history and future direction toward clinical therapy. *Neural Regen Res* 2018;13:599-608.
19. Bioactive Natural Products for Pharmaceutical Applications: Springer, Cham; 2021.
20. Kaja S, Payne AJ, Singh T, et al. An optimized lactate dehydrogenase release assay for screening of drug candidates in neuroscience. *J Pharmacol Toxicol Methods* 2015;73:1-6.
21. Xu T, Ren D, Sun X, et al. Dual roles of sulforaphane in cancer treatment. *Anticancer Agents Med Chem* 2012;12:1132-42.
22. Singh SV, Herman-Antosiewicz A, Singh AV, et al. Sulforaphane-induced G2/M phase cell cycle arrest involves checkpoint kinase 2-mediated phosphorylation of cell division cycle 25C. *J Biol Chem* 2004;279:25813-22.
23. Gamet-Payrastre L, Lumeau S, Gasc N, et al. Selective cytostatic and cytotoxic effects of glucosinolates hydrolysis products on human colon cancer cells in vitro. *Anticancer Drugs* 1998;9:141-8.
24. Chiao JW, Chung FL, Kancherla R, et al. Sulforaphane and its metabolite mediate growth arrest and apoptosis in human prostate cancer cells. *Int J Oncol* 2002;20:631-6.

25. Traka M, Gasper AV, Smith JA, et al. Transcriptome analysis of human colon Caco-2 cells exposed to sulforaphane. *J Nutr* 2005;135:1865-72.
26. Herman-Antosiewicz A, Johnson DE, Singh SV. Sulforaphane causes autophagy to inhibit release of cytochrome C and apoptosis in human prostate cancer cells. *Cancer Res* 2006;66:5828-35.
27. Lan H, Yuan H, Lin C. Sulforaphane induces p53deficient SW480 cell apoptosis via the ROSMAPK signaling pathway. *Mol Med Rep* 2017;16:7796-804.
28. Rutz J, Juengel E, Euler S, et al. Chronic Sulforaphane Application Does Not Induce Resistance in Renal Cell Carcinoma Cells. *Anticancer Res* 2018;38:6201-7.
29. Fimognari C, Hrelia P. Sulforaphane as a promising molecule for fighting cancer. *Mutat Res* 2007;635:90-104.
30. Wang Y, Wu H, Dong N, et al. Sulforaphane induces S-phase arrest and apoptosis via p53-dependent manner in gastric cancer cells. *Sci Rep* 2021;11:2504.
31. Chaitanya GV, Babu PP. Differential PARP cleavage: an indication of heterogeneous forms of cell death and involvement of multiple proteases in the infarct of focal cerebral ischemia in rat. *Cell Mol Neurobiol* 2009;29:563-73.